INTERNATIONAL JOURNAL OF COMPUTERS COMMUNICATIONS & CONTROL
Online ISSN 1841-9844, ISSN-L 1841-9836, Volume: 21, Issue: 2, Month: April, Year: 2026
Article Number: 7065, https://doi.org/10.15837/ijccc.2026.2.7065

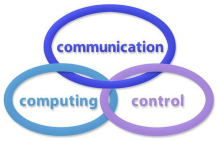

CCC Publications

Multi-objective feature selection for acute hypotension prediction models: a quantum particle swarm optimization-based study

Xiaohan Liu, Ying Li, Yuzhuo Zhao, Lijun Dong, Zihui Hong, Jing Li

Xiaohan Liu+
School of Economics and Management
Beijing Jiaotong University, Beijing, China
22120630@bjtu.edu.cn

Ying Li+
Department of Stomatology,
Fu Xing Hospital,
Capital Medical University, Beijing, China
liying5326@163.com

Yuzhuo Zhao
Department of Cardiology,
The 79th Military Hospital of the
People's Liberation Army, Liaoning, China
zhaoyuzhuo0421@126.com

Lijun Dong
Department of Cardiology,
The 79th Military Hospital of the
People's Liberation Army, Liaoning, China
dlj201ok@163.com

Zihui Hong
Department of Cardiology,
The 79th Military Hospital of the
People's Liberation Army, Liaoning, China
330544676@qq.com

Jing Li*
School of Economics and Management
Beijing Jiaotong University, Beijing, China
*Corresponding author: jingli@bjtu.edu.cn

+These authors contributed equally to this work.

Abstract

Acute hypotension is a common and severe clinical condition, closely associated with adverse outcomes such as acute kidney injury and myocardial infarction. Existing research primarily relies on vital sign data to develop predictive models; however, relying solely on these data is insufficient to fully capture the progression of the condition. Integrating laboratory biomarkers can provide a more comprehensive assessment of patient status, thereby significantly improving the model's accuracy and clinical utility. However, the vast number of available laboratory biomarkers introduces data redundancy and increases complexity, necessitating an efficient feature selection method to identify the most relevant indicators. To overcome limitations of existing methods, this study introduces a novel integration of multi-objective optimization with quantum particle swarm optimization (QPSO), significantly improving indicator selection and prediction accuracy compared to traditional methods. This method optimizes the number of indicators, patient status identification accuracy, sensitivity, and specificity, while setting different priorities for various clinical scenarios. The method was applied to the emergency database of infection patients from the Chinese People's Liberation Army General Hospital to identify key indicators that align with current clinical needs. The selected indicators demonstrated strong alignment with clinical experience and established guidelines, highlighting their clinical relevance. In the full feature scenario, the model exhibited significant improvements in accuracy, F1 score, and specificity, with accuracy ranging from 89.75%

to 94.07% and a peak specificity of 98.51%, outperforming other feature selection methods. Even in high-restriction scenarios, where fewer indicators were available, the model maintained strong performance, with accuracy ranging from 88.66% to 93.38%, demonstrating the method's resilience and reliability. The proposed multi-objective QPSO method performed excellently across different scenarios, providing an effective tool for indicator selection in acute hypotension prediction and complex medical data analysis. This method enhances the model's accuracy and clinical applicability, supporting more precise predictions and practical implementation in diverse clinical environments.

Keywords: Feature selection; Hypotension; Particle swarm optimization; Multi-objective optimization.

1 Introduction

Acute hypotensive episodes (AHE) are defined as a sudden drop in blood pressure to a systolic level below 90 mmHg, a diastolic level below 60 mmHg, or a reduction of more than 30% from a higher baseline. Alternatively, AHE may be characterized by a MAP that remains at or below 60 mmHg for more than 30 minutes [1]. AHE can be triggered by various factors, including infections, trauma, pancreatitis, and hemorrhage. Infectious diseases are often accompanied by vasodilation and hemodynamic changes, leading to significant drops in blood pressure. Prolonged hypotension can compromise organ perfusion, potentially leading to multiple organ dysfunction syndrome (MODS) and, in severe cases, life-threatening conditions[2]. Recently, numerous studies have focused on developing early warning systems for AHE using machine learning techniques, aiming to provide healthcare professionals with valuable intervention time. Most of these studies predominantly rely on vital sign data, especially blood pressure and its derived statistical features. For instance, Kendale et al.[3]developed a hypotension prediction model using preoperative medications, medical comorbidities, induction medica tions, and time-series data from intraoperative vital signs. Additionally, other research efforts[4, 5] have sought to extract features from MAP time-series waveforms to identify numerical characteristics most likely associated with AHE onset.

In clinical practice, physicians often need to consider multidimensional patient data to make comprehensive and accurate diagnostic and treatment decisions, especially when dealing with complex conditions. While vital signs data can reflect a patient's immediate physiological status, it may not always capture subtle health changes, particularly when the disease progresses insidiously[6]. In contrast, laboratory biomarkers (such as blood tests, metabolic parameters, and other lab data) provide deeper insights at the pathological level, revealing changes in cellular, organ, and metabolic functions. These data effectively complement the physiological information derived from vital signs. Therefore, integrating vital signs with laboratory biomarkers when constructing hypotension prediction models can significantly enhance the model's ability to predict patient status, offering a more comprehensive pathological context. This integration supports more precise risk assessment and treatment interventions by clinicians. The fusion of multi-source data not only improves early warning systems for acute hypotension but also lays a robust foundation for personalized medicine, facilitating the early identification of potential health risks and enabling timely and effective interventions[7].

The vast array of clinical indicators in patient data complicates rapid and accurate assessments by clinicians, underscoring the need for effective selection of key indicators. Many current studies address indicator selection as a multi-objective optimization problem, balancing between the number of features and classification errors. For instance, Jimenez et al.[8] optimized feature selection for predicting antibiotic resistance outbreaks by minimizing the number of indicators while maximizing model performance. Abd et al.[9] employed a strategy to minimize selected feature quantities while maximizing descriptor dependencies to predict risk factors in unknown biotransformation drugs. However, in the medical field, evaluation metrics beyond accuracy, such as sensitivity and specificity, are crucial[10]. Sensitivity (related to low miss rates) and specificity (related to minimizing false positives) reflect the model's ability to detect true cases without overdiagnosing, making them essential for clinical reliability. Relying solely on accuracy does not provide a comprehensive assessment of the model's performance in real-world clinical applications[11, 12]. Therefore, integrating sensitivity and specificity into multi-objective optimization not only enhances diagnostic capability but also offers

clinicians more reliable guidance for decision-making.

Existing literature predominantly employs wrapper methods for feature selection[13, 14], which integrate feature selection directly with model training, iteratively evaluating different feature subsets to identify those most critical for predictive performance. Due to their ability to align closely with the performance of the prediction model, wrapper methods are especially suited for precise feature screening and have demonstrated significant advantages in many medical prediction tasks. However, this approach requires repeated model training and evaluation of feature subsets, leading to high computational costs and complex iterations, making it time-consuming[15]. To address this issue, researchers have recently introduced meta-heuristic optimization algorithms, aiming to balance computational efficiency and model performance[16]. Among various meta-heuristic algorithms, the particle swarm optimization (PSO) algorithm has emerged as a successful nature-inspired method due to its fast convergence, flexible parameter adjustment, and strong global search capabilities[17]. The core of PSO lies in the collaboration and information sharing among particles, which enables them to iteratively approach the optimal solution. Nevertheless, classic PSO may struggle with slow convergence or getting trapped in local optima when dealing with high-dimensional, complex problems. Existing wrapper-based methods require repeated model training, resulting in high computational overhead. Unlike classical PSO, which suffers from premature convergence and local optima, our QPSO-based approach ensures better global exploration capability, significantly enhancing feature selection efficiency[18]. QPSO has been successfully applied to several complex optimization tasks, such as multi-agent system task allocation[19], fault diagnosis in mechanical transmission systems[20], and edge detection and fine segmentation in image processing[21]. These applications demonstrate QPSO's superior performance and wide adaptability. Therefore, applying QPSO to feature selection is expected to overcome the computational bottlenecks of wrapper methods in medical prediction, improving both predictive accuracy and efficiency.

To comprehensively evaluate the performance of predictive models, our study integrates multi-objective optimization concepts with QPSO algorithm, proposing a novel QPSO-based feature selection method. This approach simultaneously incorporates the number of features, accuracy of patient status recognition, sensitivity, and specificity as optimization objectives. Through this multi-objective strategy, the method not only balances the model's performance across various metrics but also allows for prioritization of goals based on different clinical scenarios, thereby catering to diverse diagnostic needs. Our research particularly focuses on two typical scenarios of acute hypotension (AHE), each reflecting distinct clinical requirements. In these settings, the model dynamically adjusts optimization targets to ensure that the selected feature set can accurately predict hypotension while also meeting practical clinical demands. By identifying and integrating key features into the hypotension prediction model, our proposed method significantly enhances both the model's accuracy and practical utility, making it more adaptable to real-world clinical settings.

2 Materials and methods

2.1 Dataset

The data for this study were obtained from the emergency database of the Chinese People's Liberation Army General Hospital, focusing on infection patients. Inclusion and exclusion criteria were established based on relevant literature[22] and guidance from emergency department physicians at the hospital(see Figure 1):

Inclusion Criteria: 1) Patients aged 18 or older with complete admission and discharge records; 2) Patients diagnosed with infections, determined through ICD-9 coding and clinical expertise; 3) Patients whose systolic blood pressure (SBP) remained $\leq$90 mmHg or decreased by 30% from baseline for over 30 minutes during hospitalization were included in the experimental group, while those with SBP consistently >90 mmHg were classified in the control group.

Exclusion Criteria: 1) Patients whose SBP dropped below 90 mmHg during hospitalization but did not last for 30 minutes were excluded; 2) Patients in the experimental group who used antihypertensive drugs or underwent surgery within 30 minutes before the onset of hypotension were excluded to ensure that the hypotensive events were spontaneous or pathophysiological in nature, thus enhancing the

clinical purity of the dataset; 3) Patients in the control group who used vasopressors or underwent surgery were excluded to avoid misclassification of individuals whose potential hypotensive episodes may have been suppressed by medical interventions.

Patients who developed acute hypotension after infection were assigned to the experimental group, while those who did not experience acute hypotension were included in the control group. The study also divided the samples into four groups based on the occurrence and duration of AHE[23]: AHE(group 1), AHE lasting 0.5-1 hour(group 2), AHE lasting 1-2 hours(group 3), and AHE lasting more than 2 hours(group 4). These classifications allowed for the analysis of physiological differences across different stages, revealing the pathophysiological mechanisms of AHE over time.

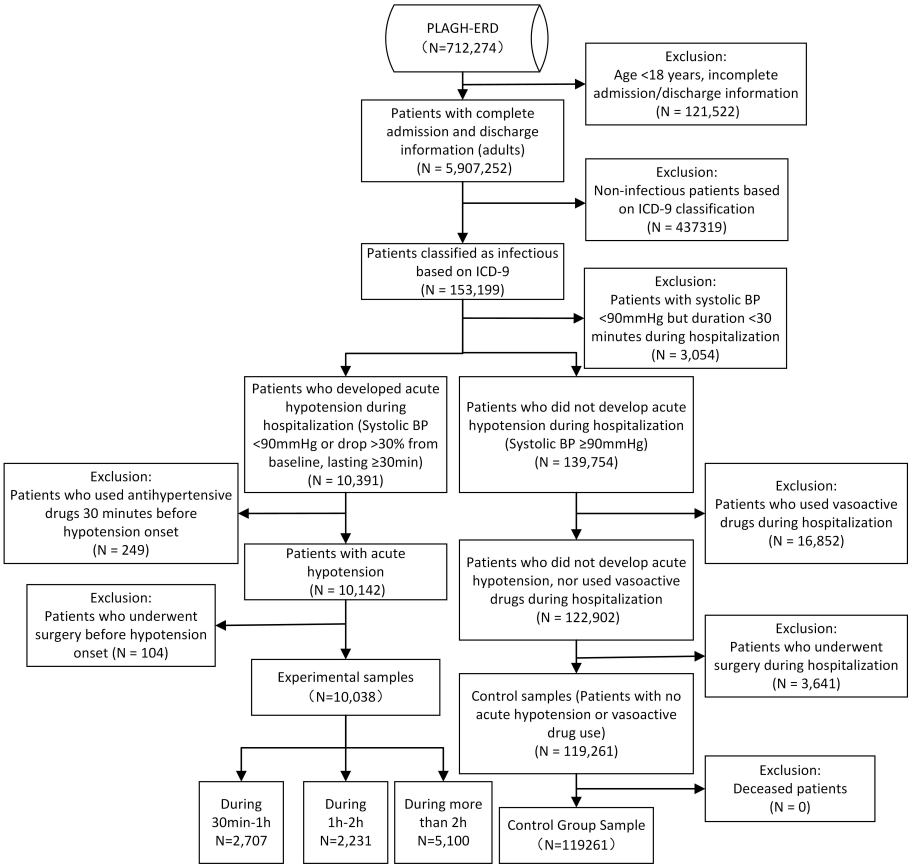

Figure 1: Inclusion and exclusion process

In selecting indicators for our study, we expanded beyond commonly used vital signs to include laboratory metrics such as blood gas analysis, complete blood count, blood biochemistry, coagulation factors, and inflammation markers. Indicators with a missing rate exceeding 80% were excluded from the dataset[24]. Ultimately, 62 indicators were retained as initial features, comprising 6 vital signs, 5 blood gas analysis indicators, 16 complete blood count metrics, 25 blood biochemistry markers, 7 coagulation function indicators, and 3 inflammation markers.

2.2 Scenario and Objective Setting

The number of features is a critical factor in optimization. Patient data often contain numerous indicators, but not all contribute significantly to predictive outcomes. By reducing redundant or irrelevant features, the model's complexity can be simplified, leading to improved computational efficiency and enabling clinicians to make faster decisions in practice. Accuracy is a core metric for assessing overall model performance, with higher accuracy reflecting stronger predictive capability. However, relying solely on accuracy can obscure the model's limitations, especially when handling different types of errors. In the medical field, overlooking sensitivity and specificity may have serious consequences[25]. Sensitivity measures the model's ability to correctly identify positive cases. Low

sensitivity can lead to missed diagnoses, causing patients to miss the optimal treatment window, potentially endangering lives. Enhancing sensitivity reduces the risk of missed diagnoses, ensuring that high-risk patients receive timely interventions. Specificity, on the other hand, indicates the model's ability to accurately identify negative cases, thereby minimizing false positives. This reduces unnecessary treatments, conserves resources, and alleviates patients' psychological burdens. Therefore, both sensitivity and specificity are essential in medical predictions and must not be overlooked.

In medical data analysis, the complexity and availability of data collection can vary significantly due to limitations imposed by different environments and equipment conditions. This diversity poses distinct challenges for model design, particularly in feature selection and optimization of predictive models. To better accommodate various clinical scenarios and enhance predictive accuracy, the experimental settings were categorized into two types based on recommendations from clinical experts at the Chinese People's Liberation Army General Hospital. These categories, termed full-feature and high-restriction scenarios, were defined by the ease of data acquisition within the patient's environment.

Full-Feature Scenario: This scenario represents environments with comprehensive equipment, such as well-equipped hospital settings. In such settings, there are fewer limitations on data collection, allowing for the acquisition of a wide range of indicators. This enables the use of complex and comprehensive feature sets for building predictive models. Here, accuracy is the primary focus, to ensure that clinicians can make more reliable diagnoses based on extensive data support. Since false positives can may lead to unnecessary medical interventions and resource consumption, specificity is also prioritized. Feature quantity is considered secondary, with an emphasis on simplifying the model while maintaining high accuracy and specificity. Consequently, the decision-making preference is set as: prioritize accuracy and specificity, followed by feature quantity.

High-Restriction Scenario: This scenario applies to environments such as pre-hospital emergency care or triage stations, where data collection equipment is limited, typically allowing only the capture of basic vital signs and blood gas indicators. Due to these equipment constraints, extensive and complex data cannot be collected, making it essential to simplify the model inputs to ensure practical applicability. In this context, the primary focus is on minimizing the number of features to reduce the complexity and time required for data collection. Additionally, the simplified data environment may increase the risk of missed diagnoses, making sensitivity a key priority to avoid missing critical hypotensive episodes. While feature quantity and sensitivity take precedence, accuracy remains an important consideration. Consequently, the decision-making preference in this scenario is to prioritize feature quantity and sensitivity, followed by accuracy.

The multi-objective problem constructed in this study is solved using the Quantum Particle Swarm Optimization (QPSO) algorithm. QPSO integrates the advantages of traditional PSO with quantum behavior characteristics, significantly enhancing the algorithm's global exploration capabilities. It addresses the common issues in traditional PSO, such as premature convergence and a tendency to get trapped in local optima. With its robust global search ability and suitability for high-dimensional problems, QPSO is particularly well-suited for the multi-objective optimization of feature selection tasks developed in this study. During the optimization process, each particle represents a combination of features encoded using quantum bits. The update of particle positions involves strategies such as quantum rotation gates, mean-variance, and chaotic mutation, allowing the algorithm to better explore the solution space and avoid local optima. Through multiple iterations, the algorithm gradually optimizes the particle swarm positions, ultimately identifying the key feature combinations that contribute most to the model's predictive performance. This optimization process not only enhances the model's predictive accuracy, but also improves its practical applicability in clinical settings.

2.3 Feature Selection Model and Pareto Optimal Solutions

For binary classification problems, metrics such as accuracy, recall, and precision are commonly used to evaluate the performance of classifiers. In the medical field, however, additional considerations are essential, particularly sensitivity and specificity[26]. High sensitivity indicates a low rate of missed diagnoses (false negatives), while high specificity reduces the rate of incorrect diagnoses (false

positives). Based on these evaluation metrics, the objective set D in this study can be defined as:

$$D = \{Accuracy, Sensitivity, Specificity, Index\}$$

where accuracy represents the overall prediction accuracy of the model, sensitivity indicates the model's ability to correctly identify true positive cases, specificity reflects the model's ability to correctly identify true negative cases.

$$Accuracy = (TN + TP)/(TN + TP + FN + FP)$$

$$Sensitivity = TP/(TP + FN)$$

$$Specificity = TN/(TN + FP)$$

In different clinical scenarios, physicians may exhibit varying decision-making preferences. As a result, the constraint set J can be defined as

$$J = \{ScenarioConstraints, DecisionPreferences\}$$

The scenario constraints and decision preferences within J influence the selection and prioritization of the objective set D. Consequently, these constraints must be associated with the objectives when constructing the optimization model. This linkage between constraints and objectives formulates a multi-objective optimization problem, as described below:

$$minf(D, J)subjecttoJ$$

In multi-objective optimization, the objectives often conflict with one another, making it challenging to optimize them simultaneously. To address this, the concept of Pareto optimality is introduced to balance multiple competing objectives effectively[27].

Definition 1: Pareto Dominance. Consider a multi-objective optimization problem with m objective functions $f_1(x), f_2(x), \ldots, f_m(x)$, collectively denoted as the objective vector $F(x) = [f_1(x), f_2(x), \ldots, f_m(x)]$. Given two objective vectors $F(x_A)$ and $F(x_B)$, we say that $F(x_A)$ dominates $F(x_B)$, written as $F(x_A) \succ F(x_B)$, if and only if: $f_i(x_A) \leq f_i(x_B)$ for all $i = 1, 2, \ldots, m$, and there exists at least one $j \in \{1, 2, \ldots, m\}$ such that $f_i(x_A) < f_i(x_B)$.

Definition 2: Pareto non-dominated solution A solution x_A in the decision space is called non-dominated if there does not exist another feasible solution x_k such that $F(x_k) \succ F(x_A)$.

Definition 3: Pareto optimal set The Pareto optimal set consists of all non-dominated solutions within the decision space, where none of the solutions can dominate another. The Pareto front refers to the set of corresponding objective function values in the objective space, representing the trade-offs among the optimal solutions.

By leveraging the concept of Pareto optimality, this study seeks to identify a set of solutions where multiple objectives are balanced, ensuring that no objective can be improved without compromising others. This approach provides a robust framework for handling conflicting objectives and supports more informed decision-making.

2.4 Execution Process of the QPSO Algorithm

Step 1: Initialization of Algorithm Parameters. The algorithm begins by initializing key parameters, including the population size N, the storage capacity for the individual non-dominated solution set ND_i within each particle, and the global non-dominated solution set ND_g. Additionally, the number of iterations is set. Each particle in the population is encoded using quantum bits x_i, and the corresponding objective function values are represented as:

$$F(x_i) = [f_1(x_i), f_2(x_i), f_3(x_i)]$$

Step 2: Evaluation of Particle Feature Sets. Each particle in the population represents a quantum bit encoding with a length m, corresponding to the number of selected features. These feature sets are used as input for the machine learning algorithm to evaluate their effectiveness. The objective

function values, derived from training the model on these feature combinations, are calculated and assessed against the solutions in the non-dominated solution sets. The process follows specific rules to update the non-dominated solution sets ND (including both ND_i and ND_g). For any solution $\mathrm{ND}(k)$ within the non-dominated set, if $F(x_i) \succ \mathrm{ND}(k)$, then $\mathrm{ND}(k)$ is removed from the set. Conversely, if $F(x_i)$ is not dominated by any existing solution in ND, it is added to the set.

Step 3: Calculation of Crowding Distance within the Non-Dominated Set. Let K represent the number of solutions stored in the non-dominated set. First, the solutions are sorted in descending order based on their objective function values $f_r(x_s)$, resulting in a new sequence with reordered indices $f'_r(x_s)$, where r denotes the objective function index (in this study, $r = 1, 2, 3$) and $s \in [1, K]$. The crowding distance for the s-th solution in objective r is calculated as follows:

$$d_{(s,r)} = \begin{cases} \frac{f'_r(x_{s+1}) - f'_r(x_{s-1})}{f'_r(x_K) - f'_r(x_1)}, & s \in (1, K) \\ \infty, & s = 1 \text{ or } s = K \end{cases}$$

The total crowding distance for the s-th solution is determined by summing over all objective functions:

$$d_s = \sum_{r=1}^{M} d_{(s,r)}$$

Step 4: Selection of "Individual Best" and "Global Best" Quantum Bit Encodings. Based on the calculated crowding distances, the algorithm selects the "individual best" quantum bit encoding from the local non-dominated set ND_i and the "global best" quantum bit encoding from the global non-dominated set ND_g. The probability of a particle being selected is proportional to its crowding distance, where particles with larger crowding distances have a higher likelihood of being chosen. The probability for selection is computed as the ratio of the particle's crowding distance to the total crowding distance of all particles. The particle chosen from ND_i is denoted as i', while the particle selected from ND_g is represented as i''.

Step 5: Deriving Optimal Encodings Using Mean-Variance Method and Updating Particles via Quantum Rotation Gate. The process begins by converting the current quantum bit encoding of particle i, along with its "individual best" and "global best" encodings, into real-number encodings. Let these be denoted as $x_i^R, x_{i'}^R$, and $x_{i''}^R$, respectively, where

$$x_i^R = \{x_{i1}^R, \ldots, x_{ik}^R, \ldots, x_{im}^R\}.$$

The mean and variance are calculated as $\mu_i^R = (x_{i'}^R + x_{i''}^R)/2$ and $\sigma = |x_{i'}^R - x_{i''}^R|$, respectively. The optimal encoding x_i^{R*} is then derived using the mean-variance crossover operator:

$$x_i^{R*} = N(\mu_i^R, \sigma^2)$$

Next, a random number rand is generated within the range $[0, 1]$. If rand $< p_s$ (where p_s is the probability of selecting the particle update method), the algorithm compares $F(x_i^R)$ and $F(x_i^{R*})$ and designs a rotation angle adjustment strategy: $\theta_{ik} = \Delta\theta_{ik} \cdot s(\alpha_{ik}, \beta_{ik})$. Here, $\Delta\theta_{ik}$ denotes the rotation angle, and $s(\alpha_{ik}, \beta_{ik})$ indicates the direction of rotation. The adjustment strategy is determined, after which the particle's flight position is updated based on the rules detailed in the Table 1.

Table 1: Quantum Rotation Adjustment Strategy

x_{ik}	μ_{ik}	$F(x_i^R) \succ F(x_i^{(R*)})$	$\alpha_{ik} \cdot \beta_{ik} > 0$	$\alpha_{ik} \cdot \beta_{ik} < 0$	$\alpha_{ik} = 0$	$\beta_{ik} = 0$
0	1	False	1	-1	0	±1
0	1	True	-1	1	±1	0
1	0	False	-1	1	±1	0
1	0	True	1	-1	0	±1

Step 6: Chaotic Mutation. To introduce further variability, a mutation probability p_m is set. Particles are selected for mutation with a probability of p_m. For each chosen particle i, the variable x_{ik}^R undergoes t iterations using the Tent map. The iterative process is defined as:

$$x_{ik}^R(t+1) = \begin{cases} 2x_{ik}^R(t), & \text{if } x_{ik}^R(t) \leq 0.5, \\ 2 - 2x_{ik}^R(t), & \text{if } x_{ik}^R(t) > 0.5. \end{cases}$$

Step 7: Termination Condition. The algorithm concludes when the Pareto front no longer changes or when the maximum number of iterations is reached. If this condition is not met, the process loops back to Step 2.

It is important to note that since QPSO is a heuristic algorithm, the Pareto front obtained represents a set of approximate non-dominated solutions identified through iterative search, rather than the theoretical global Pareto-optimal front. Despite this, the algorithm effectively approximates the Pareto front of key feature combinations, providing balanced trade-offs across multiple clinical criteria. Moreover, the objective function priorities can be flexibly adjusted based on specific scenario constraints and decision-making preferences. This allows the algorithm to guide the selection of clinically relevant feature sets that align with the most critical objectives in each clinical scenario.

3 Result

3.1 Results of Hypotension Indicator Selection

In full-feature scenario, where comprehensive monitoring equipment is available, the system can collect most of the necessary indicators, enabling the use of a full set of indicators as inputs for the multi-objective model. Based on the decision preference, which prioritizes accuracy and specificity over the number of indicators, the model selects the combination from the Pareto-optimal solutions that offers the highest accuracy, as shown in Table 2. From the table, it can be observed that the key indicators chosen across the four groups of post-infection AHE samples include MAP, Lac, HR, LDH, and DBIL, among others, indicating their critical role in the onset and progression of AHE[28, 29]. As illustrated in the accompanying Figure 2, indicators associated with cardiovascular function are more prominent in the early stages of AHE[30]. However, as the duration of AHE extends, the selected indicators shift towards those reflecting more severe physiological disruptions, such as inflammation and coagulation abnormalities. For patients experiencing prolonged AHE, emphasis is placed on markers related to myocardial injury and systemic inflammatory responses, including troponin T, procalcitonin, and C-reactive protein[31, 32]. In the early stages of hypotension, various organs and tissue cells may begin to experience different degrees of ischemia and hypoxia. For example, sensitive vital signs such as HR and MAP often show early fluctuations, while Lac, an indicator of microcirculatory dysfunction, tends to rise concurrently. These key indicators are consistently present across all feature sets. Clinically, a prolonged duration of hypotension typically indicates greater difficulty in correction, reflecting more severe underlying conditions and associated with progressive organ hypoperfusion and cellular injury. In Group 2, early elevations in ALT, CREA, and CK likely reflect the high sensitivity of the liver, kidneys, and muscles to ischemic and hypoxic insults. In Group 4, cTnT shows a marked increase, and the average CREA level is higher than that in Group 2 (127.9 vs. 106.9 umol/L). Other vital signs, including RR and Temp, also exhibit deteriorating trends. These findings suggest that myocardial and renal injury may already be present prior to the onset of hypotension, indicating more advanced disease severity.

These observations align with established clinical understanding and further support the clinical validity and pathophysiological relevance of the model's selected features.

Table 2: Full-feature scenario Select indicators

Group 1 (24)	MAP, Lac, NT-proBNP, HR, BMI, LDH, SpO2, PTA, DBIL, RBC, pCO2, AST, D-Dimer, MCHC, NEU, PT, MONO, K+, CK, GGT, CO2, BE, Pi, EOC
Group 2 (22)	MAP, NT-proBNP, Lac, LDH, HR, SpO2, PTA, DBIL, NEU, WBC, pO2, GGT, CO2, MCV, IL-6, PLT, K+, CK, MONO, CREA, ALT, Mg
Group 3 (21)	MAP, BUN, Lac, HR, DBIL, PTA, D-Dimer, LYM, WBC, pCO2, CK-MB, HCT, INR, pO2, CO2, PLT, TP, PH, FIB, MCH, BASO
Group 4 (22)	MAP, Lac, HR, LDH, cTnT, PCT, Mb, TT, PTA, TBIL, RR, SpO2, CRP, HCT, GLU, temp, MPV, PH, CREA, MCV, CO2, EOC

In our study, the selected indicators were categorized into six groups: vital signs, complete blood count (CBC), blood biochemistry, blood gas, coagulation function, and inflammatory markers. To evaluate the importance of each category for the model's predictive performance, we employed SHAP (Shapley Additive Explanations) values to quantify the contribution of each indicator to the model's

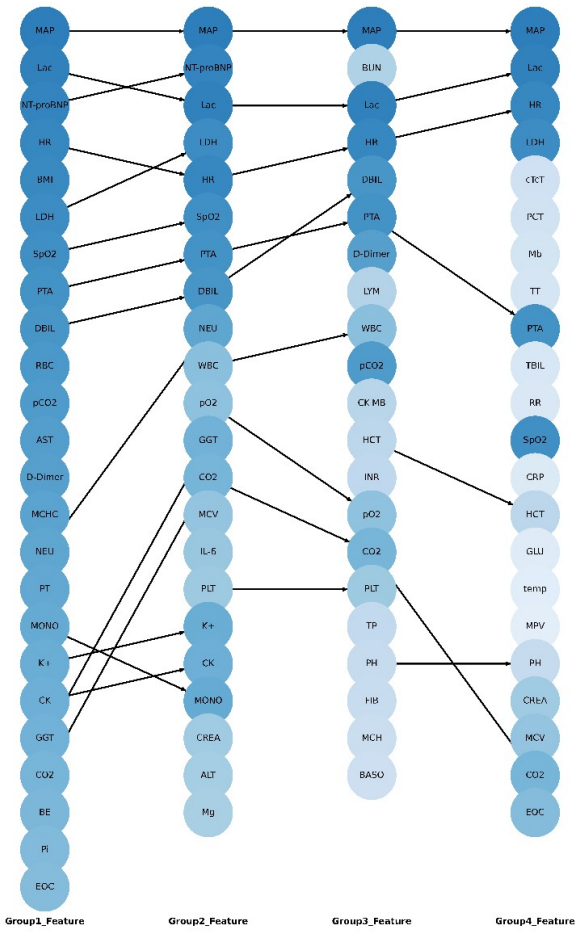

Figure 2: Full-feature scene feature directed graph

output. SHAP values, derived from the Shapley value principle in game theory, aim to explain the predictions made by machine learning models[33]. By calculating the marginal contribution of a feature across all possible feature combinations, SHAP reveals its overall influence on the model's output, with each feature's SHAP value indicating its positive or negative impact. Summing the SHAP values within each category allowed us to determine their relative importance in the model[34]. The results(see Table 3) demonstrated that, in addition to vital signs, blood biochemistry and blood gas indicators also significantly contributed to the predictive performance, highlighting the critical role of incorporating laboratory test data in the model.

Table 3: Sum the SHAP values of different types of indicators

Category	**Group 1**	**Group 2**	**Group 3**	**Group 4**
Vital Signs	0.2463	0.1231	0.0976	0.1892
Blood Biochemistry	0.1527	0.1089	0.0651	0.1084
Blood Gas	0.0931	0.0391	0.0504	0.0628
CBC	0.0510	0.0351	0.0338	0.0292
Coagulation	0.0424	0.0116	0.0318	0.0315
Inflammatory Indicators	0	0.0056	0	0.0336

In the high-restriction scenario, where equipment limitations necessitate reducing the complexity of data collection, the primary objective was to minimize the number of selected indicators. Based on the cumulative SHAP values from the Full-feature scenario, we determined that selecting only vital signs, blood biochemistry, and blood gas indicators would retain the most significant predictive features. However, blood biochemistry indicators often require longer processing times, making them less suitable for rapid decision-making in this context. Following discussions with clinical experts, it

was concluded that vital signs and blood gas indicators would be the most appropriate input features for the model in this scenario. Additionally, to prioritize patient safety and reduce the risk of missed diagnoses, the study aimed to ensure timely clinical intervention. Therefore, within the final Pareto optimal set, the combination of indicators with the highest sensitivity was selected as the optimal solution(see Table 4).And it can be intuitively seen from Figure 3 the changes of the indicators selected for different groups.

Among the indicators chosen across the four groups of post-infection AHE samples, systolic blood pressure (SBP), diastolic blood pressure (DBP), lactate (Lac), and heart rate (HR) were ranked as the most critical. HR and blood pressure-related indicators such as SBP and DBP are widely recognized as key markers for detecting hypotension[35]. Lactate, a product of tissue hypoxia and anaerobic metabolism, increases under hypotensive conditions due to insufficient tissue perfusion, forcing cells to rely more on anaerobic pathways. Elevated lactate levels are closely associated with shock and organ dysfunction[36].

Table 4: Full-feature scenario Select indicators

Group 1 (8)	SBP, HR, Lac, SpO2, RR, temp, pCO2, PH
Group 2 (8)	SBP, HR, SpO2, RR, temp, pO2, pCO2, PH
Group 3 (8)	SBP, HR, DP, Lac, SpO2, temp, pO2, PH
Group 4 (8)	SBP, DP, HR, Lac, RR, SpO2, temp, PH

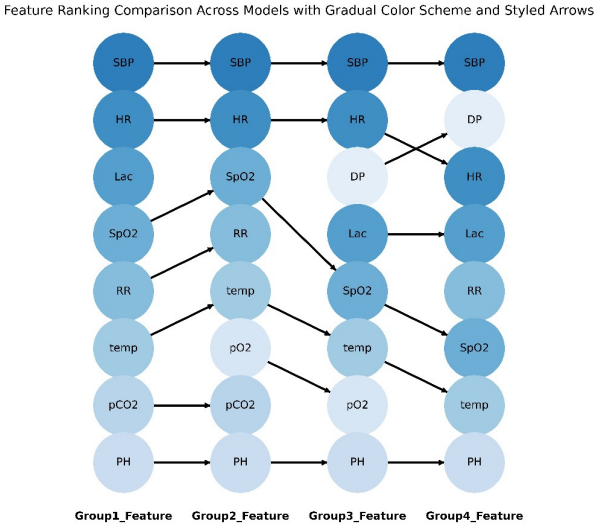

Figure 3: Full-feature scene feature directed graph

To further analyze the relationship between the selected features and the final predictive outcomes, this study employed the SHAP (Shapley Additive Explanations) method for feature importance interpretation[37]. By visualizing SHAP bee swarm plots, the overall impact and marginal contribution of each feature to the model's output were intuitively displayed(see Figure 4 and Figure 5). The horizontal axis in the plots represents the SHAP values, which indicate how each feature affects the model's predictions: a larger SHAP value suggests that the feature is likely to increase the prediction, while a smaller SHAP value implies the opposite. Each point on the plot corresponds to the SHAP value of a particular sample for a given feature, with color gradients reflecting the feature's actual value—blue indicating lower values and red denoting higher values. The combination of color and SHAP values allows for a clear illustration of how variations in feature values influence the model's predictions, enhancing the interpretability of the model. Additionally, the bee swarm plots reveal similarities and differences in feature influence across various scenarios, providing insights into the model's dependencies and decision-making processes. This enhanced interpretability offers a clearer reference for understanding the model's behavior in practical applications.

The selected indicators identified through our research were compared with clinical guidelines and expert opinions. This comparison revealed that the features deemed highly significant by our study align closely with established clinical knowledge, demonstrating clear clinical relevance(see Table 5).

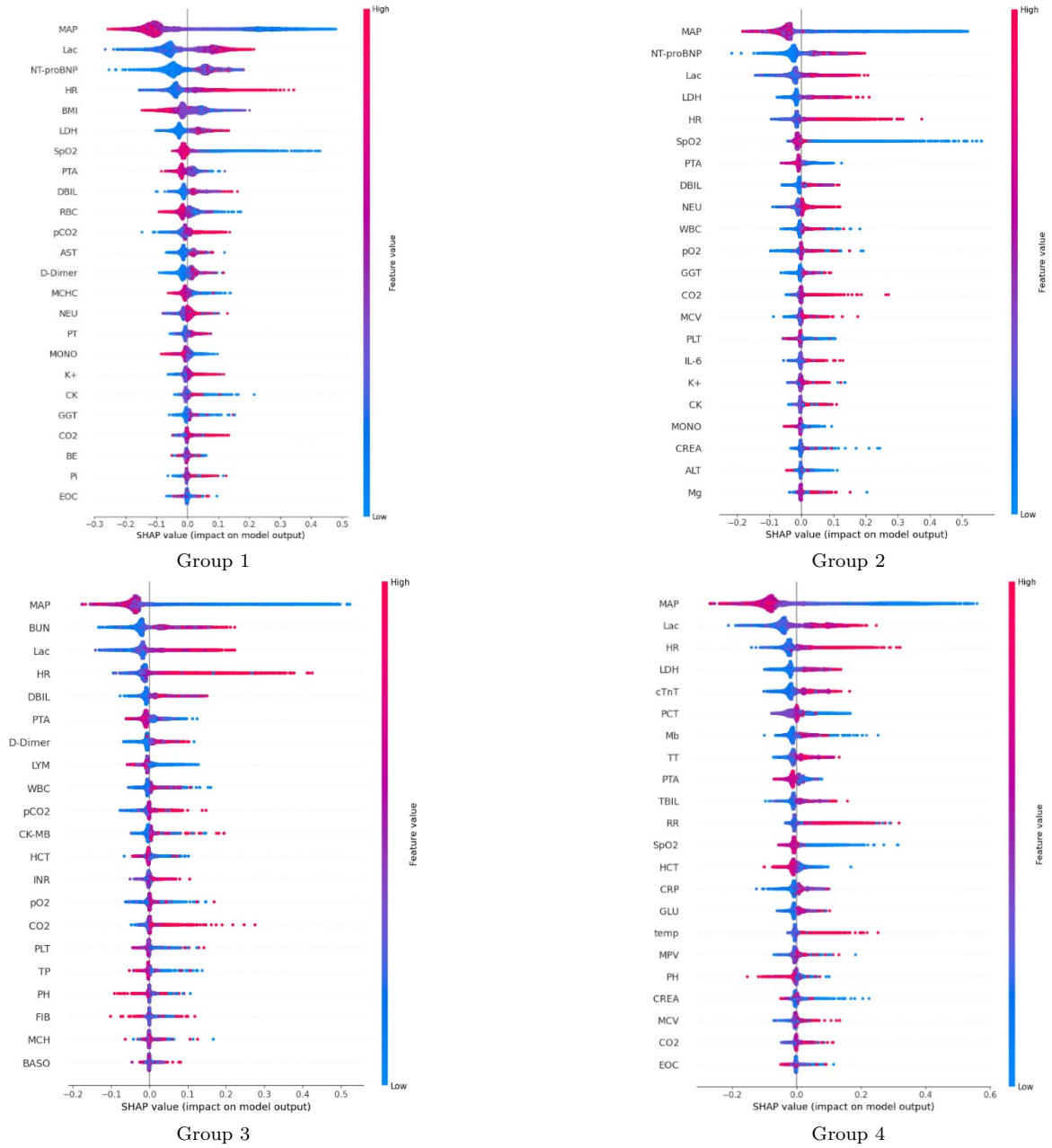

Figure 4: SHAP cellular diagram of each sample in the full-feature scenario

3.2 Results Comparison

To evaluate the performance of the proposed multi-objective QPSO algorithm in feature selection, this study compared it against four commonly used feature selection methods: filter-based methods (correlation matrix and mutual information), wrapper methods (recursive feature elimination with cross-validation, RFECV), and embedded methods (Gini impurity-based selection).

Correlation matrix-based feature selection quantifies the linear relationship between each feature and the target variable by calculating correlation coefficients, retaining highly correlated features while eliminating those with low correlation or high multicollinearity[38]. The mutual information method, on the other hand, captures both linear and nonlinear dependencies by measuring the mutual information between features and the target, selecting features that contribute the most information gain[39]. The RFECV method recursively constructs models to eliminate the least significant features, using cross-validation to ensure the selected features generalize well[40]. Finally, Gini impurity-based selection, employed in decision tree models (such as random forests), identifies features that maximize data purity, thereby pinpointing those that most significantly contribute to the target variable[41].

After applying these four methods to filter 62 features, a random forest model was constructed,

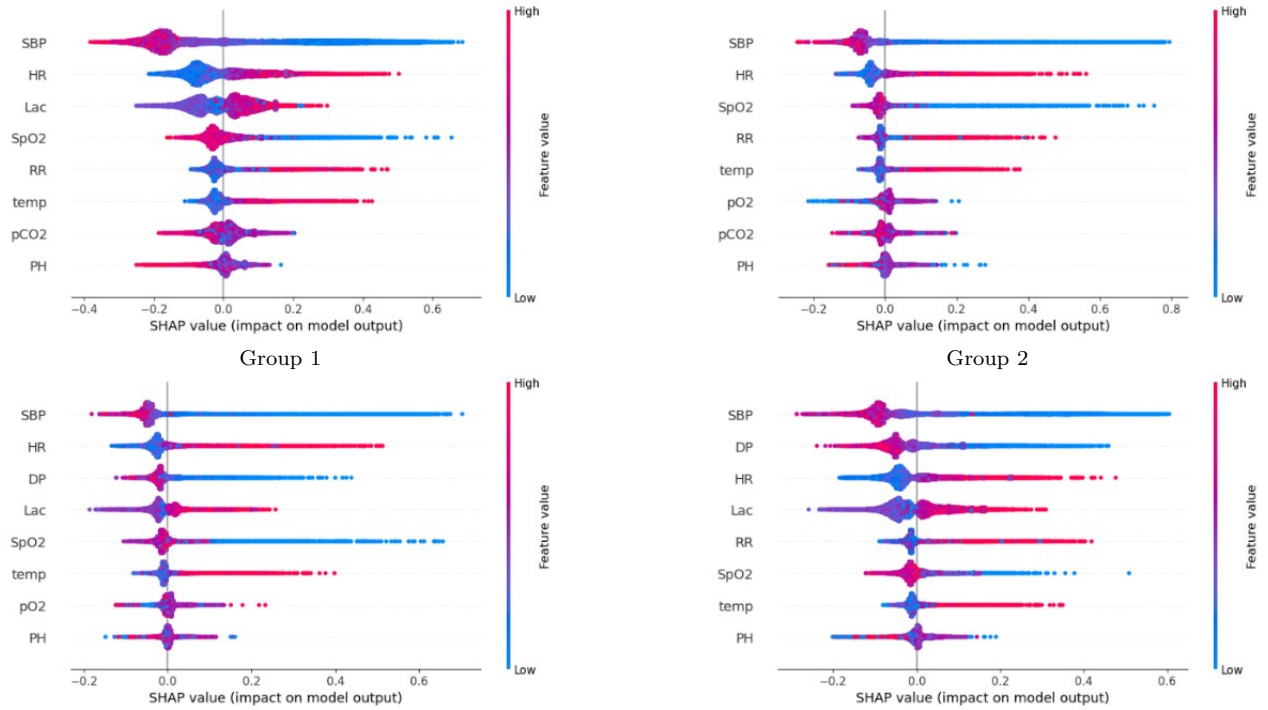

Figure 5: SHAP cellular diagram of each sample in a high-restriction scenario

Table 5: Clinical significance of the selected indicators

Indicator	Clinical Significance
MAP	A critical hemodynamic parameter, directly reflecting the perfusion status of vital organs.
Lactate	A byproduct of anaerobic metabolism; elevated during AHE due to insufficient tissue perfusion, leading to lactate accumulation.
HR	Tachycardia may be a compensatory response to maintain cardiac output during AHE.
SpO2	Low oxygen saturation indicates severe hypoperfusion and oxygen transport dysfunction, closely related to AHE progression.
DBIL	Elevated levels indicate liver dysfunction, which can impair systemic metabolism and immune regulation, thereby increasing AHE risk.
LDH	A marker of cell damage; hypoxia and hypoperfusion during AHE cause cell damage and necrosis, leading to elevated LDH levels.
PTA	Decreased prothrombin activity suggests coagulation abnormalities, which may lead to bleeding or thrombosis, exacerbating systemic hypoperfusion and increasing the risk of AHE.
pCO2	Variations in pCO2 levels indicate disturbances in the body's acid-base balance.
NT-proBNP	A biomarker released by the heart in response to volume overload or cardiac stress, associated with the onset of hypotension following infection.

and performance was evaluated using metrics such as accuracy, precision, F1-score, sensitivity, and specificity[42].

$$precision = TP/(TP + FN)$$

$$F1 = 2 * precision * recall/(precision + recall)$$

The results(see Table 6)demonstrate that the QPSO algorithm outperformed other feature selection methods across all key metrics, including accuracy, precision, specificity, and sensitivity, exhibiting robust overall performance.

To demonstrate the overall superiority of the proposed method, we employed radar charts to visualize the model's performance metrics(see Figure 6). This allowed for a comprehensive comparison across multiple evaluation dimensions and provided an intuitive illustration of the method's balanced optimization capability.

In high-restriction scenarios, the selection of easily accessible indicators such as vital signs and blood gas parameters, followed by multi-objective feature selection, effectively reduced the complexity of the model while maintaining acceptable performance, as shown in Table 7. Despite the reduction

Table 6: Performance comparison result

Group	Method	Accuracy	Precision	F1 Score	Sensitivity	Specificity
Group 1	QPSO	**0.8975**	**0.8921**	**0.8601**	0.8302	**0.9386**
	RFECV	0.8928	0.8814	0.8530	0.8263	0.9329
	Mutual Information	0.8952	0.8749	0.8568	**0.8394**	0.9285
	Correlation matrix	0.8722	0.8601	0.8237	0.7903	0.9220
	Gini impurity	0.8900	0.8805	0.8485	0.8189	0.9329
Group 2	QPSO	**0.9326**	**0.8421**	**0.7095**	0.6130	**0.9822**
	RFECV	0.9231	0.8125	0.6667	0.5652	0.9795
	Mutual Information	0.9262	0.8350	0.6995	0.6018	0.9802
	Correlation matrix	0.9270	0.8117	0.6920	0.6030	0.9780
	Gini impurity	0.9252	0.8219	0.7040	**0.6157**	0.9775
Group 3	QPSO	**0.9407**	**0.8442**	**0.7066**	**0.6076**	**0.9851**
	RFECV	0.9367	0.8338	0.6970	0.5987	0.9835
	Mutual Information	0.9335	0.8428	0.6802	0.5702	0.9849
	Correlation matrix	0.9343	0.7908	0.6603	0.5667	0.9810
	Gini impurity	0.9388	0.8155	0.6848	0.5902	0.9831
Group 4	QPSO	**0.9256**	**0.8971**	**0.8285**	0.7696	**0.9731**
	RFECV	0.9235	0.8782	0.8248	**0.7774**	0.9675
	Mutual Information	0.9191	0.8716	0.8181	0.7709	0.9649
	Correlation matrix	0.9015	0.8580	0.7713	0.7005	0.9640
	Gini impurity	0.9185	0.8621	0.8120	0.7675	0.9634

Table 7: High-restriction scenario model performance

Group	Accuracy	Precision	F1 Score	Sensitivity	Specificity
Group 1	0.8866	0.8695	0.8458	0.8234	0.9250
Group 2	0.9218	0.8024	0.6866	0.6000	0.9754
Group 3	0.9338	0.8249	0.6890	0.5915	0.9822
Group 4	0.9162	0.8703	0.8055	0.7498	0.9663

in the number of features, the decline in model performance remained within an acceptable range. This finding suggests that using vital signs and blood gas indicators not only provides strong representativeness and predictive capability but also offers sufficient information for the effective prediction and management of AHE. Moreover, this approach simplifies data collection processes, reduces the complexity of clinical operations, and enhances the applicability and practicality of the model in real-world medical settings. This is particularly beneficial in clinical scenarios where rapid decision-making is critical.

4 Discussion

We integrated multi-objective optimization concepts with the QPSO algorithm to propose a novel feature selection method based on multi-objective QPSO. This approach incorporates feature count, prediction accuracy, sensitivity, and specificity as optimization targets. The multi-objective optimization strategy not only enables a balanced performance across different evaluation metrics but also allows the prioritization of objectives based on specific clinical scenarios, ensuring the method can be tailored to diverse diagnostic needs.

Our study focuses on two typical AHE scenarios, each corresponding to distinct clinical requirements. Based on the characteristics of these scenarios, the optimization objectives can be dynamically adjusted, ensuring that the selected feature sets accurately predict patients' hypotensive states while aligning with practical clinical needs. Results indicate that as AHE progresses, the importance ranking of indicators exhibits a phased shift. For instance, during short-term AHE episodes (lasting 0.5-1 hour), cardiovascular-related indicators such as MAP and HR are predominant. However, as the duration of AHE increases, the model increasingly emphasizes indicators reflecting more severe physiological disruptions and organ dysfunction, such as Lac, cTnT, and PCT. This progression reveals the pathological evolution of AHE from hemodynamic instability to systemic inflammation and organ failure, aligning with previous studies which indicate that the consequences of AHE worsen with longer durations[43].

In the full-feature scenario, comprehensive data collection was enabled by advanced equipment, allowing the model to prioritize accuracy, specificity, and streamlined feature selection, resulting in

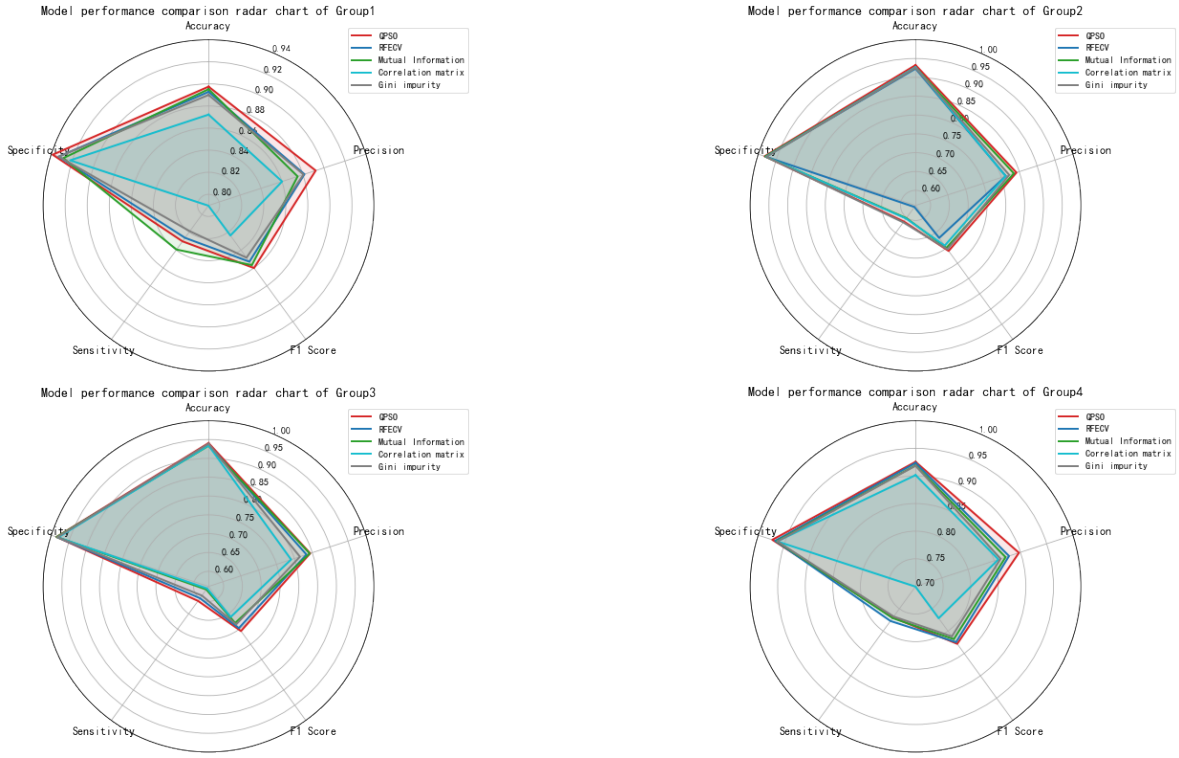

Figure 6: SHAP cellular diagram of each sample in the full-feature scenario

superior predictive performance. The study demonstrated that model accuracy ranged from 89.75% to 94.07%, with specificity reaching up to 98.51%. These results align with the findings of Sun et al., where incorporating multiple physiological indicators enhanced predictive performance[44].

In the resource-constrained scenario, equipment limitations necessitated the retention of only vital signs and blood gas parameters. Despite the reduced input data, the model maintained robust performance, with accuracy ranging from 88.66% to 93.38%. This suggests that in resource-limited settings, simplified feature sets can sustain predictive power while significantly enhancing data collection and processing efficiency, making the approach especially valuable for emergency and rapid decision-making scenarios. SHAP analysis further confirmed that these streamlined feature sets effectively predict AHE occurrence and duration. Even with limited equipment, the simplified features reliably provided accurate predictions.

In general, our feature selection strategy effectively integrates clinical requirements and equipment constraints, demonstrating broad applicability and practical potential in various scenarios. However, this study has certain limitations. The experimental data were derived from a single-center dataset collected at the Chinese People's Liberation Army General Hospital, which may limit the generalizability of the proposed QPSO-based feature selection method. Future research should involve multicenter and geographically diverse datasets to further validate the robustness and applicability of the approach. Moreover, the dynamic nature of physiological states may affect the model's generalization capability. Our current model is constructed based on static features and does not fully capture temporal changes during disease progression. To address this, future work could explore the incorporation of temporal modeling techniques, such as time series analysis or adaptive mechanisms like dynamic windowing, to enhance the model's responsiveness to complex clinical situations and improve its predictive performance and generalizability.

5 Conclusion

We integrate multi-objective optimization concepts with QPSO to develop an innovative feature selection method. By constructing multi-objective models and analyzing prediction requirements for two typical scenarios, we precisely defined optimization objectives and balanced competing goals to

achieve comprehensive optimization across diverse needs. In the full-feature scenario, the method substantially improved the model's capacity to detect AHE, effectively supporting clinicians in identifying high-risk patients early, reducing misdiagnoses and unnecessary interventions, and optimizing the allocation of medical resources. In high-restriction scenarios, simplified combinations of vital signs and blood gas indicators maintained reliable performance even with limited data, making the method particularly suitable for pre-hospital triage, emergency transport, and time-sensitive decision-making environments.

Compared with conventional feature selection methods, our approach achieves superior clinical performance across all major metrics. Moreover, by incorporating SHAP analysis for interpretability, the method enables transparent explanation of each indicator's contribution to prediction outcomes, thus improving clinicians' trust and acceptance of model decisions. From a clinical impact perspective, this method offers practical value for risk warning and personalized management of hypotensive patients. On one hand, it enables earlier prediction of AHE—often before overt symptoms appear—facilitating proactive intervention and risk stratification. On the other hand, its flexible model design and feature adaptability promote deployment across diverse clinical departments and use cases, enhancing system-wide decision-making support.

In summary, the proposed approach serves not only as a technically advanced predictive tool but also as a clinically actionable solution. It provides a new pathway for integrating AI-driven feature selection into complex medical prediction tasks and holds significant promise for improving rapid recognition and decision-making in acute and critical care settings.

Funding

This work was funded by the Beijing Outstanding Young Scientist Program.

Author contributions

Xiaohan Liu and Ying Li contributed equally to this work and share first authorship. Xiaohan Liu proposed the research methodology and conducted data analysis. Ying Li provided the data screening criteria and explained the rationale behind the selection of clinical indicators. Yuzhuo Zhao supplied the data used in this study and interpreted the experimental results. Lijun Dong, and Zihui Hong assisted in data processing and experiment implementation. Jing Li guided the development of the research methodology and contributed to the interpretation of the results.

Conflict of interest

The authors declare no conflict of interest.

References

[1] J.C. Jentzer, B. Burstein, S. Van Diepen, J. Murphy, D.R. Holmes Jr, M.R. Bell, G.W. Barsness, T.D. Henry, V. Menon, C.S, Rihal. Defining shock and preshock for mortality risk stratification in cardiac intensive care unit patients, *Circulation: Heart Failure*, DOI: https://doi.org/10.1161/CIRCHEARTFAILURE.120.007678, 14(1), e007678, 2021.

[2] M Cherifa, A Blet, A Chambaz, E Gayat, M Resche-Rigon, R Pirracchio. Prediction of an acute hypotensive episode during an ICU hospitalization with a super learner machine-learning algorithm, *Anesthesia & Analgesia*, DOI: https://doi.org/10.1213/ANE.0000000000004539, 130(5), 1157–1166, 2020.

[3] S. Kendale, P. Kulkarni, A. D. Rosenberg, and J. Wang. Supervised Machine-learning Predictive Analytics for Prediction of Postinduction Hypotension, *Anesthesiology*, DOI: https://doi.org/10.1097/ALN.0000000000002374, 129(4), 675–688, 2018.

[4] H. Galeana-Zapién, E. Aldana-Bobadilla, J. Arciniegas-García, J. Vargas-Gómez, J. Villalobos-Silva. A flexible framework for coding and predicting acute hypotensive episodes using Markov chains, *Knowledge-Based Systems*, DOI: https://doi.org/10.1016/j.knosys.2023.111237, 284, 111237, 2024.

[5] D. Jiang, G. Tu, D. Jin, K. Wu, C. Liu, L. Zheng, T. Zhou. A hybrid intelligent model for acute hypotensive episode prediction with large-scale data, *Information Sciences*, DOI: https://doi.org/10.1016/j.ins.2020.08.033, 546, 787-802, 2021.

[6] M. Cherifa, Y. Interian, A. Blet, M. Resche-Rigon, R. Pirracchio. The Physiological Deep Learner: First application of multitask deep learning to predict hypotension in critically ill patients, *Artificial Intelligence in Medicine*, DOI: https://doi.org/10.1016/j.artmed.2021.102118, 118, 102118, 2021.

[7] X. Wang, R. Zhang, B. Zhao, Y. Yao, H. Zhao, X. Zhu. Medical knowledge graph completion via fusion of entity description and type information, *Artificial Intelligence in Medicine*, DOI: https://doi.org/10.1016/j.artmed.2024.102848, 151, 102848, 2024.

[8] F. Jimenez, J. Palma, G. Sanchez, D. Marin, M.F. Palacios, M.L. López. Feature selection based multivariate time series forecasting: An application to antibiotic resistance outbreaks prediction, *Artificial Intelligence in Medicine*, DOI: https://doi.org/10.1016/j.artmed.2020.101818, 104, 101818, 2020.

[9] M. Abd Elaziz, Y.S. Moemen, A.E. Hassanien, S. Xiong. Toxicity risks evaluation of unknown FDA biotransformed drugs based on a multi-objective feature selection approach, *Applied Soft Computing*, DOI: https://doi.org/10.1016/j.asoc.2019.105509, 97, 105509, 2020.

[10] Y. Kumar, S. Gupta, R. Singla, Y.C. Hu. A systematic review of artificial intelligence techniques in cancer prediction and diagnosis, *Archives of Computational Methods in Engineering*, DOI: https://doi.org/10.1007/s11831-021-09648-w, 29(4), 2043-2070, 2022.

[11] X. Chen, M. Zhou, Z. Wang, S. Lu, S. Chang, Z. Zhou. Immunotherapy treatment outcome prediction in metastatic melanoma through an automated multi-objective delta-radiomics model, *Computers in Biology and Medicine*, DOI: https://doi.org/10.1016/j.compbiomed.2021.104916, 138, 104916, 2021.

[12] N. Binney, C. Hyde, P.M. Bossuyt. On the origin of sensitivity and specificity, *Annals of internal medicine*, DOI: https://doi.org/10.7326/M20-5028, 174(3), 401-407, 2021.

[13] M. Rostami, K. Berahmand, E. Nasiri, S. Forouzandeh. Review of swarm intelligence-based feature selection methods, *Engineering Applications of Artificial Intelligence*, DOI: https://doi.org/10.1016/j.engappai.2021.104210, 100, 104210, 2021.

[14] B.H. Nguyen, B. Xue, M. Zhang. A survey on swarm intelligence approaches to feature selection in data mining, *Swarm and Evolutionary Computation*, DOI: https://doi.org/10.1016/j.swevo.2020.100663, 54, 100663, 2020.

[15] B. Nouri-Moghaddam, M. Ghazanfari, M. Fathian. A novel multi-objective forest optimization algorithm for wrapper feature selection, *Expert Systems with Applications*, DOI: https://doi.org/10.1016/j.eswa.2021.114737, 175, 114737, 2021.

[16] M. Abdel-Basset, W. Ding, D. El-Shahat. A hybrid Harris Hawks optimization algorithm with simulated annealing for feature selection, *Artificial Intelligence Review*, DOI: https://doi.org/10.1007/s10462-020-09860-3, 54(1), 593-637, 2021.

[17] M. Marufuzzaman, M.A. Timu, J. Sarkar, A. Islam, L.F Rahman, L.M. Sidek. Multi objective PSO with passive congregation for load balancing problem, *International Journal of Computers Communications & Control*, DOI: https://doi.org/10.15837/ijccc.2021.5.4274, 16(5), 4274, 2021.

[18] G. He, X. Lu. Quasi opposite-based learning and double evolutionary QPSO with its application in optimization problems, *Engineering Applications of Artificial Intelligence*, DOI: https://doi.org/10.1016/j.engappai.2023.106861, 126, 106861, 2023.

[19] M. Li, C. Liu, K. Li, X. Liao, K. Li. Multi-task allocation with an optimized quantum particle swarm method, *Applied Soft Computing*, DOI: https://doi.org/10.1016/j.asoc.2020.106603, 96, 106603, 2020.

[20] W. Deng, H. Liu, J. Xu, H. Zhao, Y. Song. An improved quantum-inspired differential evolution algorithm for deep belief network, *IEEE Transactions on Instrumentation and Measurement*, DOI: https://doi.org/10.1109/TIM.2020.2983233, 69(10), 7319-7327, 2020.

[21] H Verma, D Verma, PK Tiwari. A population based hybrid FCM-PSO algorithm for clustering analysis and segmentation of brain image, *Expert systems with applications*, DOI: https://doi.org/10.1016/j.eswa.2020.114121, 167, 114121, 2021.

[22] S. Ghosh, J. Li, L. Cao, K. Ramamohanarao. Septic shock prediction for ICU patients via coupled HMM walking on sequential contrast patterns, *Journal of biomedical informatics*, DOI: https://doi.org/10.1016/j.jbi.2016.12.010, 66, 19-31, 2017.

[23] J. Schenk, M. Wijnberge, J.M. Maaskant, M.W. Hollmann, L. Hol, R.V. Immink, A.P. Vlaar, B.J. van der Ster, B.F. Geerts, D.P. Veelo. Effect of Hypotension Prediction Index-guided intraoperative haemodynamic care on depth and duration of postoperative hypotension: A sub-study of the Hypotension Prediction trial, *British journal of anaesthesia*, DOI: https://doi.org/10.1016/j.bja.2021.05.033, 127(5), 681-688, 2021.

[24] M. Kazijevs, M.D. Samad. Deep imputation of missing values in time series health data: A review with benchmarking, *Journal of biomedical informatics*, DOI: https://doi.org/10.1016/j.jbi.2023.104440, 144, 104440, 2023.

[25] K.J. van Stralen, V.S. Stel, J.B. Reitsma, F.W. Dekker, C. Zoccali, and K.J. Jager. Diagnostic methods I: sensitivity, specificity, and other measures of accuracy, *Kidney international*, DOI: https://doi.org/10.1038/ki.2009.92, 75(12), 1257-1263, 2009.

[26] M. Mahmood, K. Alsalem, M. Elbashir, S. Abd El-Ghany, A. Abd El-Aziz. Acute knee injury detection with magnetic resonance imaging (MRI), *International Journal of Computers Communications & Control*, DOI: https://doi.org/10.15837/ijccc.2024.5.6648, 19(5), 6648, 2024.

[27] N. Mladenovic, B. Stanojević. Solution Algorithm Involving Heuristics and Criterion Set Dissection to Solve Large Scale Multicriteria Knapsack Problems, *International Journal of Computers Communications & Control*, https://doi.org/10.15837/ijccc.2026.1.7267, 21(1), 7267, 2026.

[28] N. Jagan, L.E. Morrow, R.W. Walters, R.W. Plambeck, T.M. Patel, D.R. Moore, M.A. Malesker. Sympathetic stimulation increases serum lactate concentrations in patients admitted with sepsis: implications for resuscitation strategies, *Annals of Intensive Care*, DOI: https://doi.org/10.1186/s13613-021-00805-9, 11, 1-9, 2021.

[29] S.J. Davies, S.T. Vistisen, Z. Jian, F. Hatib, T.W. Scheeren. Ability of an arterial waveform analysis–derived hypotension prediction index to predict future hypotensive events in surgical patients, *Anesthesia & Analgesia*, DOI: https://doi.org/10.1213/ane.0000000000004121, 130(2), 352-359, 2020.

[30] L. Meng. Heterogeneous impact of hypotension on organ perfusion and outcomes: a narrative review, *British journal of anaesthesia*, DOI: https://doi.org/10.1016/j.bja.2021.06.048, 127(6), 845-861, 2021.

[31] M. Stocker, W. van Herk, S. El Helou, S. Dutta, F.A. Schuerman, R.K. van den Tooren-de Groot, J.W. Wieringa, J. Janota, L.H. van der Meer-Kappelle, R. Moonen. C-reactive protein,

procalcitonin, and white blood count to rule out neonatal early-onset sepsis within 36 hours: a secondary analysis of the neonatal procalcitonin intervention study, *Clinical Infectious Diseases*, DOI: https://doi.org/10.1093/cid/ciaa876, 73(2), e383-e390, 2021.

[32] S. Vallabhajosyula, A. Sakhuja, J.B. Geske, M. Kumar, J.T. Poterucha, R. Kashyap, K. Kashani, A.S. Jaffe, J.C. Jentzer. Role of Admission Troponin-T and Serial Troponin-T Testing in Predicting Outcomes in Severe Sepsis and Septic Shock, *Journal of the American Heart Association*, DOI: https://doi.org/10.1161/JAHA.117.005930, 6(9), e005930, 2017.

[33] X. Wang, R. Zhang, X. Zhu. What can we learn from multimorbidity? A deep dive from its risk patterns to the corresponding patient profiles, *Decision Support Systems*, DOI: https://doi.org/10.1016/j.dss.2024.114313, 186, 114313, 2024.

[34] A. Nayebi, S. Tipirneni, C.K. Reddy, B. Foreman, V. Subbian. WindowSHAP: An efficient framework for explaining time-series classifiers based on Shapley values, *Journal of biomedical informatics*, DOI: https://doi.org/10.1016/j.jbi.2023.104438, 144, 104438, 2023.

[35] J.H. Yoon, V. Jeanselme, A. Dubrawski, M. Hravnak, M.R. Pinsky, G. Clermont. Prediction of hypotension events with physiologic vital sign signatures in the intensive care unit, *Critical Care*, DOI: https://doi.org/10.1186/s13054-020-03379-3, 24, 1-9, 2020.

[36] G.L. Sacha, S.W. Lam, L. Wang, A. Duggal, A.J. Reddy, S.R. Bauer. Association of catecholamine dose, lactate, and shock duration at vasopressin initiation with mortality in patients with septic shock, *Critical care medicine*, DOI: https://doi.org/10.1097/ccm.0000000000005317, 50(4), 614-623, 2022.

[37] W. Huang, H. Suominen, T. Liu, G. Rice, C. Salomon, A.S. Barnard. Explainable discovery of disease biomarkers: The case of ovarian cancer to illustrate the best practice in machine learning and Shapley analysis, *Journal of biomedical informatics*, DOI: https://doi.org/10.1016/j.jbi.2023.104365, 141, 104365, 2023.

[38] M Kushwaha, M.S. Abirami. Intelligent Model for Avoiding Road Accidents Using Artificial Neural Network, *International Journal of Computers Communications & Control*, DOI: https://doi.org/10.15837/ijccc.2023.5.5317, 18(5), 5317, 2023.

[39] X. Song, Y. Zhang, D. Gong, X. Sun. Feature selection using bare-bones particle swarm optimization with mutual information, *Pattern Recognition*, DOI: https://doi.org/10.1016/j.patcog.2020.107804, 112, 107804, 2021.

[40] W. Liu, J. Wang. Recursive elimination–election algorithms for wrapper feature selection, *Applied Soft Computing*, DOI: https://doi.org/10.1016/j.asoc.2021.107956, 113, 107956, 2021.

[41] S.K. Trivedi. A study on credit scoring modeling with different feature selection and machine learning approaches, *Technology in Society*, DOI: https://doi.org/10.1016/j.techsoc.2020.101413, 63, 101413, 2020.

[42] Y. Chen, K. Chen. MADMN: A Multi-modal Attention and Dynamic Memory Network for Early Mortality Risk Prediction in Electronic Medical Records, *International Journal of Computers Communications & Control*, DOI: https://doi.org/10.15837/ijccc.2025.3.6968, 20(3), 6968, 2025.

[43] K. Maheshwari, B.H. Nathanson, S.H. Munson, V. Khangulov, M. Stevens, H. Badani, A.K. Khanna, D.I. Sessler. The relationship between ICU hypotension and in-hospital mortality and morbidity in septic patients, *Intensive care medicine*, DOI: https://doi.org/10.1007/s00134-018-5218-5, 44, 857-867, 2018.

[44] Y. Sun, N. Rashedi, V. Vaze, P. Shah, R. Halter, J.T. Elliott, N.A. Paradis. Predicting future occurrence of acute hypotensive episodes using noninvasive and invasive features, *Military Medicine*, DOI: https://doi.org/10.1093/milmed/usaa418, 186(Supplement_1), 445-451, 2021.

Journal's webpage: http://univagora.ro/jour/index.php/ijccc/

This journal is a member of, and subscribes to the principles of,
the Committee on Publication Ethics (COPE).
https://publicationethics.org/members/international-journal-computers-communications-and-control

Cite this paper as:

Xiaohan Liu, Ying Li, Yuzhuo Zhao, Lijun Dong, Zihui Hong, Jing Li. (2026). Multi-objective feature selection for acute hypotension prediction models: a quantum particle swarm optimization-based study, *International Journal of Computers Communications & Control*, 21(2), 7065, 2026.
https://doi.org/10.15837/ijccc.2026.2.7065